

## FLUORESCENCE PROPERTIES OF $\text{As}_2\text{S}_3$ GLASS DOPED WITH RARE-EARTH ELEMENTS

M. Iovu\*, A. Andriesh, I. Culeac

Center of Optoelectronics of the Institute of Applied Physics Academy of Sciences of Moldova, NR 1 Academiei St., Chisinau MD-2028, Republic of Moldova

Chalcogenide glasses doped with various rare-earth ions are extensively studied as potential materials for fiber optic amplifiers operating at 1.3 and 1.5  $\mu\text{m}$  telecommunication windows. The experimental results on optical absorption and photoluminescence of arsenic sulfide glasses and optical fibers doped with rare-earth elements ( $\text{Pr}^{3+}$ ,  $\text{Sm}^{3+}$ ,  $\text{Er}^{3+}$  and  $\text{Dy}^{3+}$ ) are presented. Near the absorption edge the rare-earth impurities affect strongly the slope and the magnitude of the weak absorption tail. Fluorescence spectra of bulk samples and optical fibers of arsenic sulfide doped with different concentrations of  $\text{Pr}^{3+}$  and  $\text{Dy}^{3+}$  indicate on the presence of luminescent band located around 1.3 and 1.5  $\mu\text{m}$ . These bands correspond to the electron transitions from the discrete levels ( ${}^6\text{F}_{7/2} \rightarrow {}^6\text{H}_{13/2}$  and  ${}^6\text{F}_{5/2} \rightarrow {}^6\text{H}_{11/2}$  for  $\text{Dy}^{3+}$  and  ${}^1\text{G}_{4/1} \rightarrow {}^3\text{H}_6$  and  ${}^3\text{F}_3 \rightarrow {}^3\text{H}_4$  for  $\text{Pr}^{3+}$ , respectively), and which confirmed the presence of trivalent rare-earth ions in the glass matrix. The observed effects of rare-earth dopants on the  $\text{As}_2\text{S}_3$  glass are discussed in connection with the expected behavior of the impurities in the glass.

(Received May 20, 2005; accepted September 22, 2005)

*Keywords:* Chalcogenide glasses, Rare earth elements, Photoluminescence, Optical fibers.

### 1. Introduction

Glassy  $\text{As}_2\text{S}_3$  and  $\text{As}_2\text{Se}_3$  are promising candidates for optoelectronics applications because of its high transmission in the infrared (up to 10  $\mu\text{m}$ ), high refractive index ( $n \approx 2.4$ ) and low phonon energy [1-2]. The bandgap of  $\text{As}_2\text{S}_3$  lies in the visible region of the spectrum ( $E_g \approx 2.4$  eV), and thus optical transitions involving conduction bands and edge tail states overlap with some absorption/emission bands due to the discrete levels of the rare-earth ions [3]. For this reason, the photon energy absorbed in the broad band region in rare earth doped  $\text{As}_2\text{S}_3$  glasses is partially transferred to rare earth ions, and this results in the enhancement of the pumping efficiency of luminescence. This is an important effect for application in fibre optics amplifiers operating at 1.3  $\mu\text{m}$  and 1.5  $\mu\text{m}$  telecommunication windows.

Optical fibers amplifiers are the key devices for increasing the transmission distance, speed and capacity of optical communication systems. Optical fibers amplifier based on rare-earth doped chalcogenide glasses are potential candidates for the communication systems and satisfy all the main requirements: high output power and low noise, a broad gain spectrum, high reliability, low costs and compactness [4-6].

The aim of this paper is to study the effect of rare-earth ion doping ( $\text{Dy}^{3+}$  and  $\text{Pr}^{3+}$ ) on optical absorption and photoluminescence of  $\text{As}_2\text{S}_3$  glass. Because of their low photon energy, good chemical stability, easy fiber fabrication and large glass formation regions along with their extended infrared transmission out to 12  $\mu\text{m}$ , chalcogenide glasses have been selected as host materials in order to enhance the emission efficiency of the luminescence at mid-infrared wavelengths. Compared to germanium sulfide based glasses arsenic sulfide based glasses show very good glass stability. Some data on X-ray diffraction experiments, IR and Raman spectroscopy were used to reveal changes in the short range order glass structure.

\* Corresponding author: iovu@as.md

## 2. Experimental

The chalcogenide glasses of  $\text{As}_2\text{S}_3$  doped with rare-earth ions were synthesised using elements of 6N (As, S) and oxides  $\text{Dy}_2\text{O}_3$  (99.9 % (REO) and  $\text{Pr}_6\text{O}_{11}$  (99.996 % (REO)), supplied by Alfa Aesar. The conventional melting in evacuated ( $p \sim 10^{-5}$  Torr) and sealed silica ampoules was carried out at two temperature steps, 600–650 °C for 2 h and 800–850 °C for 8 h, and was followed by quenching in cold water. The nominal concentration of rare-earth ions in glass was from 0.05 up to 0.5 at.%. The bulk glasses were cut into plates of 1.5–10 mm thickness and then polished to yield samples with high quality flat surfaces suitable for optical measurements. Unclad optical fibres from arsenic sulfide doped glasses  $\text{As}_2\text{S}_3 + 0.5\%$  Pr have been obtained by a crucible technique by drawing from the melt in a gas atmosphere. The crucible assembly was charged with glass, then it was placed in an electric furnace under an Ar-gas atmosphere and then heated to 400–450 °C. The drawn fibers were 50–150  $\mu\text{m}$  in diameter.

Transmission spectra of optical fibers has been measured in a range 0.6–1.9 eV using a cut-back method. Optical losses are determined by the relation:  $\alpha = L^{-1} \ln(I_0/I)$ , where  $I_0$  is the intensity of probing light at the output end of the fibre before cutting;  $I$  – is the intensity of the probing light at the output end of the fibre after cutting;  $L$  – is the length of cut segment of the fibre. For probing light 1.15  $\mu\text{m}$  optical losses represented some 0.4  $\text{cm}^{-1}$ .

The luminescence spectra of  $\text{As}_2\text{S}_3$  bulk glasses doped with rare-earth ions were investigated, when excited by an infrared LED 90RTM 5070,  $\lambda_{\text{max}}=0.95 \mu\text{m}$  ( ${}^6\text{H}_{15/2} \rightarrow {}^6\text{F}_{7/2}$  for  $\text{Dy}^{3+}$ ). Fluorescence spectra of bulk glass samples and optical fibers were measured with a computer-driven monochromator and a selective lock-in amplifier arrangement. Two excitation light sources were used: a diode laser ИЛПН 500 ( $\lambda = 0.808 \mu\text{m}$ ) and an infrared LED 90RTM 5070 ( $\lambda = 0.95 \mu\text{m}$ ). The luminescence spectra were measured in a spectral region between 1.0 and 1.7  $\mu\text{m}$  at room temperature.

## 3. Results and discussion

### 3.1. Absorption spectra in $\text{As}_2\text{S}_3$ glasses

In chalcogenide glasses the absorption edge is broader than in crystalline analogues and this is caused by a broad energy distribution of electronic states in the band gap due to disorder and defects. The absorption edge in the high absorption region ( $\alpha > 10^4 \text{ cm}^{-1}$ ) is described by a quadratic function

$$\alpha \propto \frac{1}{h\nu} (h\nu - E_g)^2, \quad (1)$$

and when plotted in the Tauc co-ordinates  $(\alpha \cdot h\nu)^{1/2}$  vs.  $(h\nu)^4$  it gives the value of the optical gap ( $E_g$ ), determined as the energy difference between the onsets of exponential tails of the allowed conduction bands [8]. For amorphous  $\text{As}_2\text{S}_3$  the value of band gap was found [9] to be  $E_g = 2.35 \pm 2.4 \text{ eV}$ .

The optical gap  $E_g$  determined for thin film samples by extrapolation of the straight-line portions of the  $(\alpha \cdot h\nu)^{1/2}$  vs.  $(h\nu)$  graphs was found to be 2.34 eV for  $\text{As}_2\text{S}_3$  [10] and is in good agreement with previously reported data. Doping  $\text{As}_2\text{S}_3$  glass with metal impurities was found to decrease  $E_g$ , with the new optical gap value being dependent on the nature and concentration of the metal ion dopant [10].

Absorption coefficient spectra,  $\alpha$ , of bulk glasses were calculated from transmittance,  $T$ , and reflectance,  $R$ , measurements according to:

$$\alpha = \frac{-\ln T}{d} + \frac{2 \ln(1-R)}{d}, \quad (2)$$

where  $d$  is the thickness of the sample, and are shown in Fig. 1 for pure  $\text{As}_2\text{S}_3$  and  $\text{As}_2\text{S}_3+0.1 \text{ at.}\%$  Dy. In the Urbach edge region ( $\alpha \approx 1 \pm 10^3 \text{ cm}^{-1}$ ) the absorption coefficient depends exponentially on the photon energy:

$$\alpha \propto \exp\left(\frac{h\nu}{\Delta_1}\right), \quad (3)$$

where  $\Delta_1$  is the parameter which characterises the distribution of localised states in the band gap. In this region the experimentally obtained  $\alpha$  spectrum for vitreous As<sub>2</sub>S<sub>3</sub> is similar to that reported earlier [11]. In addition, the  $\Delta_1$  value for amorphous As<sub>2</sub>S<sub>3</sub> found in this work,  $\Delta_1 = 0.056$  eV, is in good agreement with the reported [11] value of 0.05 eV, whereas for As<sub>2</sub>S<sub>3</sub> doped with Dy and Sm  $\Delta_1$  is found to be somewhat higher (0.11 and 0.07 eV, respectively). For As<sub>2</sub>S<sub>3</sub> doped samples, the absorption coefficient in this region is higher (Fig. 1). The broadening of the Urbach tail is caused probably by the formation of new impurity metal-based structural units, which add compositional disorder to the existing structural disorder. The reason for such behaviour and the role of disorder in the formation of the Urbach edge is still under discussion [12].

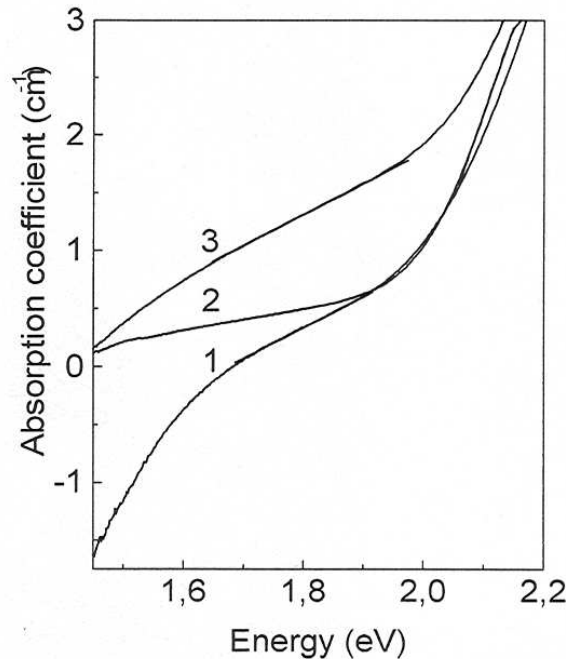


Fig. 1. The absorption coefficient spectra of bulk glasses of As<sub>2</sub>S<sub>3</sub> (1), As<sub>2</sub>S<sub>3</sub>+0.1 at.%Sm (2), and As<sub>2</sub>S<sub>3</sub>+0.1 at.%Dy (3).

The absorption coefficient spectra in the region of weak absorption ( $\alpha < 1$  cm<sup>-1</sup>) are also included in Fig. 1 and show that doping with Sm and Dy results in an increase of the absorption coefficient. It is known that in this region, the absorption coefficient depends strongly on the conditions of sample preparation and the impurities present, and this is often described by an exponential dependence:

$$\alpha \propto \exp\left(\frac{h\nu}{\Delta_2}\right), \quad (4)$$

where  $\Delta_2 > \Delta_1$  [7]. The value of  $\Delta_2$  for vitreous As<sub>2</sub>S<sub>3</sub> obtained in this work is  $\Delta_2 \approx 0.31$  eV, and this is in good agreement with the reported [9] value of 0.3 eV. Doping As<sub>2</sub>S<sub>3</sub> was found to affect drastically  $\Delta_2$  and increase up to 1.02 eV for As<sub>2</sub>S<sub>3</sub>+0.1 at.% Sm.

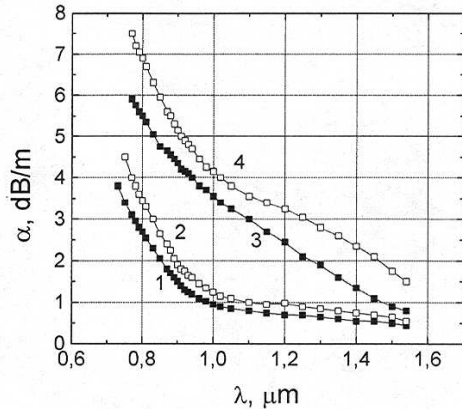


Fig. 2a. Spectral distribution of optical absorption in  $\text{As}_2\text{S}_3$  glass unclad fibres under different conditions<sup>10</sup>: (1) measured under monochromatic and (2) integral probing light; (3) under lateral illumination; (4) under neutron irradiation.

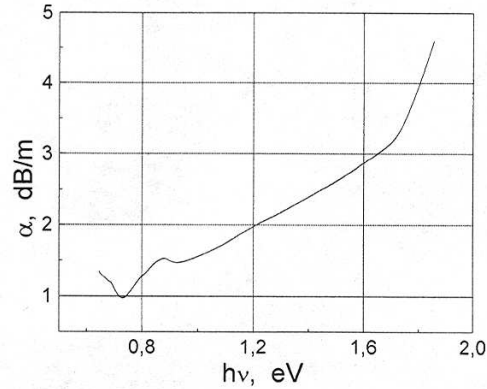


Fig. 2b. Room temperature absorption spectrum in purified  $\text{As}_2\text{S}_3$  glass fibre sample<sup>10</sup>.

The mid-IR transmission spectra of  $\text{As}_2\text{S}_3$ ,  $\text{As}_2\text{S}_3 + 0.1$  at.% Dy, and  $\text{As}_2\text{S}_3 + 0.1$  at.% Sm glasses have been reported earlier and are characterized by several well resolved absorption bands [9]. These bands are situated in the wavelengths 7560–11880 nm (As-OH), 6690 nm (O-H), 4020 nm (S-H), and 2760 nm (O-H). For  $\text{As}_2\text{S}_3 + 0.5$  at.% Sm glass additional absorption bands were registered at 4950 and 6330  $\text{cm}^{-1}$ . The observed changes upon doping in the mid infrared region are most likely related to interactions of a portion of the introduced metal ion impurities with the inherent impurities of the host glass, such as hydrogen and oxygen atoms. Such interactions result in the reduction of the relative intensity of bands associated with O-H, S-H, As-O and As-H bonds in the parent glass. Optical transmission in the weak absorption tail is affected by the extrinsic factors: lateral illumination, neutron irradiation, etc. (Fig. 2a).

The nature of the weak absorption tail in chalcogenide glasses remains to be investigated. It was demonstrated that the absorption in this spectral region is sensitive to impurities, though the weak absorption tail is still observed [13] in specially purified samples (Fig. 2b). This weak absorption may be attributed to additional states created by defects and/or impurities, or to the increase in the average amplitude of the internal electric fields produced by the introduction of additional charged centres. The latter interpretation can be applied to the present case since Sm, Pr or Dy dopants enter the host glass as three- and two-fold charged ions, respectively. It should be noted that the  $\text{As}_2\text{S}_3$  glass studied in this work shows absorption in the spectral region under consideration which is about an order of magnitude higher than that of specially purified samples employed for fibre-optic applications. Spectral distribution of optical absorption in Pr-doped  $\text{As}_2\text{S}_3$  glass fibres used for fluorescent measurements has been measured in the range 1.0–1.7  $\mu\text{m}$  (Fig. 3). One can notice several absorption bands caused by Pr dopants at 1.2, 1.35 and 1.57  $\mu\text{m}$ .

Additional treatment of glasses by irradiation for 6 hours and annealing at 210  $^\circ\text{C}$  was found to cause no significant changes in the IR transmission spectra. This fact determines stability of  $\text{As}_2\text{S}_3$ -based bulk glasses towards thermal and visible light-irradiation treatments. However, a recent study of bulk  $\text{As}_2\text{S}_3$  glass has shown that wavelength-selective infrared irradiation can cause a significant reduction of the intensity of vibrational modes associated with  $\text{CH}_x$  impurities [14]. Thus, the method of wavelength-selective infrared irradiation may provide a novel non-thermal treatment for the reduction of IR absorption attributed to impurities in  $\text{As}_2\text{S}_3$ -based glasses.

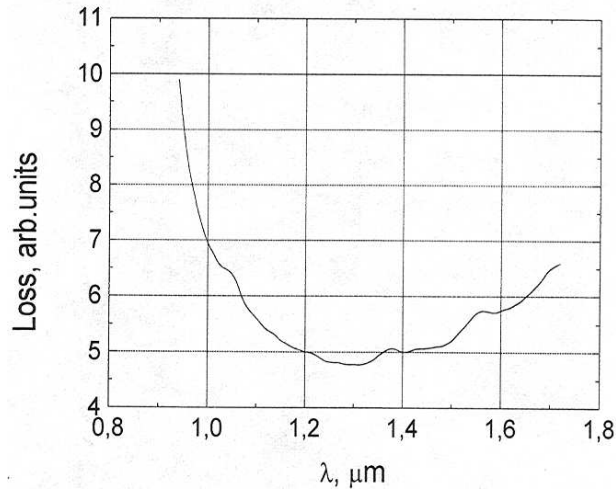


Fig. 3. Optical loss spectral distribution in chalcogenide glass fibers  $\text{As}_2\text{S}_3 + 0.5$  at. % Pr.

### 3.2. Luminescence spectra in $\text{As}_2\text{S}_3$ doped glasses

Room temperature fluorescence spectra in bulk glass samples were obtained in the IR by pumping the glass samples at  $0.95 \mu\text{m}$  with a LED. The emission from the samples were passed through a grating monochromator and detected with a Ge photodiode. The fluorescence spectrum of  $\text{As}_2\text{S}_3$  bulk glass samples doped with different rare-earth elements is shown in Fig. 3. Two quite smooth luminescence bands located around  $1.3 \mu\text{m}$  and  $1.5 \mu\text{m}$  can be observed. The full width at the half maximum (FWHM) is about  $100 \text{ nm}$ . The luminescence bands can be assigned to the electron transitions between the discrete levels of  $\text{Pr}^{3+}$  ions (Fig. 4).

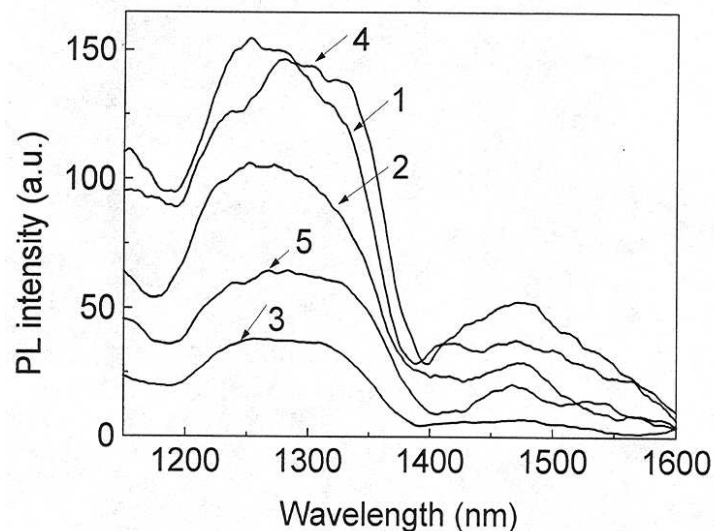


Fig. 3. The luminescence spectra of  $\text{As}_2\text{S}_3+0.15$  at.% Pr (1),  $\text{As}_2\text{S}_3+0.25$  at.% Pr (2),  $\text{As}_2\text{S}_3+0.5$  at.% Pr (3),  $\text{As}_2\text{S}_3+0.5$  at.% Dy (4), and  $\text{As}_2\text{S}_3+0.1$  at.% Er (5). Excitation light source was a LED ( $\lambda=0.95 \mu\text{m}$ ).

The analogous fluorescence band around  $1.3 \mu\text{m}$  was observed in  $\text{As}_2\text{S}_3$  samples doped with  $500 \text{ wt. ppm Pr}^{3+}$  ions, and attributed to  ${}^1\text{G}_4 \rightarrow {}^3\text{H}_5$  emission electron transitions [15]. It was found that the emission lifetime of  $250 \mu\text{s}$  decrease markedly at concentration of  $\text{Pr}^{3+}$  more than  $500 \text{ ppm}$ .

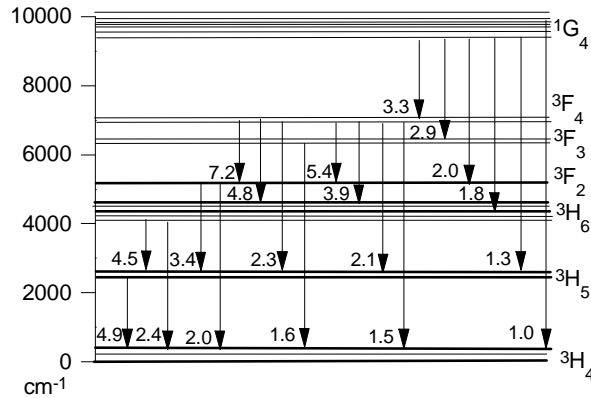


Fig. 4. Energy level diagram of  $\text{Pr}^{3+}$  ion showing possible infrared emission transitions [15].

In fibre sample  $\text{As}_2\text{S}_3 + 0.5\% \text{Pr}$  under the excitation of  $0.95 \mu\text{m}$  light the luminescence spectra exhibits a wide shaped maximum that is positioned at approximately  $1.28 \mu\text{m}$  (Fig. 5), and its amplitude represents about 1% of the maximum amplitude of the pumping light beam. Like for the bulk samples in the case of optical fiber samples  $\text{As}_2\text{S}_3 + 0.5\% \text{Pr}$  the shape of the luminescence spectra is quite wide with no signs of the amplification effect. Fluorescence centered at  $1.28 \mu\text{m}$  is associated with the  $^1\text{G}_4 \rightarrow ^3\text{H}_5$  transition and is quite smooth over this band (Fig. 4).

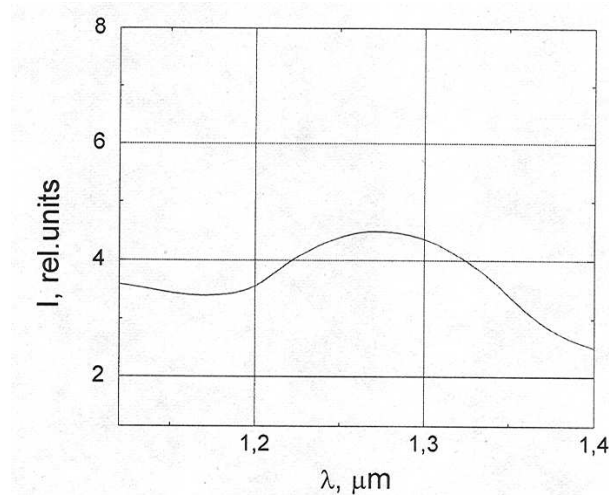


Fig. 5. Luminescence spectra in an  $\text{As}_2\text{S}_3$  glass fibre doped with 0.5% Pr at room temperature  $T = 300 \text{ K}$ . The excitation light source was a LED at  $0.95 \mu\text{m}$ .

When optical fibre sample is excited with a light beam  $0.808 \mu\text{m}$  the luminescence spectra exhibits a narrow band positioned at approximately  $1.6 \mu\text{m}$  (Fig. 6). The full width of the luminescence spectra at half maximum is some 40 nm. Fluorescence at  $1.6 \mu\text{m}$  is associated with the  $(^3\text{F}_3, ^3\text{F}_4) \rightarrow ^3\text{H}_4$  transitions.

In the case of excitation with the laser with wavelength of  $1.02 \mu\text{m}$ , the sulphide fibers doped with  $\text{Pr}^{3+}$  ions show a luminescence band located at around  $1.35 \mu\text{m}$  [16,17].

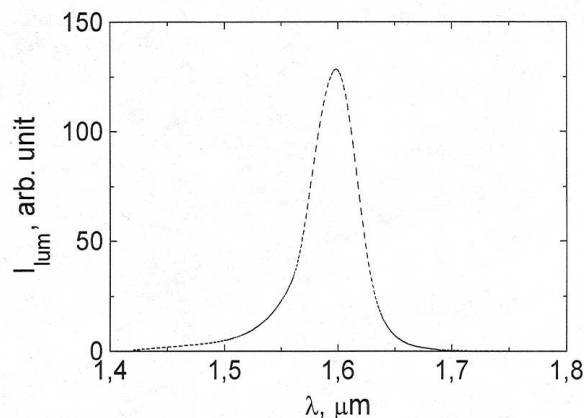


Fig. 6. Spectral distribution of the photoluminescence in  $\text{As}_2\text{S}_3$  chalcogenide glass fibers doped with 0.5% Pr. The excitation light source was a diode laser ( $\lambda = 0.808 \mu\text{m}$ ).

One should be noted that after switching on the excitation light the luminescence signal at 1.6  $\mu\text{m}$  shows pronounced time decay (Fig. 7). The fluorescence decay was measured by pumping the fibre sample at 0.808  $\mu\text{m}$  with a diode laser ИЛПН 500. The dependence of the PL signal on the time after switching on the excitation light exhibits an exponential character.

Recently investigations of photoluminescence and photoluminescence excitation spectra in Er-doped glasses show that the same native defects which cause the broad mid-gap host glass photoluminescence are also responsible for the broad band photoluminescence emission of the rare earth [18,19]. The broad band excitation process in chalcogenide glasses doped with rare earth ions was interpreted in terms of the Mott-Davis-Street model for the optical and electronic properties of native defect states [20-22].

According to this model the exciting light absorbed in the Urbach tail of the absorption edge creates an electron-hole pair in the glass. The hole is then captured by a nearby defect state (a charged dangling bond in the Mott-Davis-Street model) thereby changing the charge state of the defect. Capturing of the hole on the defect state leads to relaxation of the lattice around the defect and shifts the defect energy state deeper into the gap. The electron can then either recombine radiatively with the bound hole, giving rise to the host glass luminescence, or recombine non-radiatively, transferring its energy to a nearby rare earth atom and placing it in an excited state. Another possibility is that the pair could recombine non-radiatively, transferring its energy to the host lattice resulting in no luminescence. The third process of non-radiative recombination of the excited electron-hole pair is supposed to give rise to a broad band excitation of the rare earth dopants. This model explains the decrease in the host glass photoluminescence intensity with increasing of rare earth concentration in the hole spectral range<sup>16</sup>.

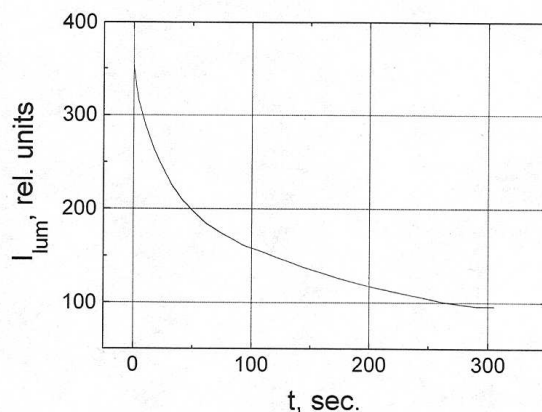


Fig. 7. The decay of photoluminescence signal ( $\lambda = 1.6 \mu\text{m}$ ) in  $\text{As}_2\text{S}_3$  glass fibers doped with 0.5% Pr after switching on the excitation light  $\lambda = 0.808 \mu\text{m}$ .

The energy transfer between the rare earth ions through different mechanisms (resonant energy transfer, stepwise upconversion, cooperative luminescence, cooperative energy transfer and simultaneous photon absorption) also must be taken into account. Although when the local concentration of rare earth ions become high enough, each ion is no longer an isolated ion that act independently of its neighbors. Sometimes the local structure in the bulk glass and optical fiber can vary, and some clustering in different region takes place. In this case, the photoluminescence spectra and life time of the relaxation process can differ in bulk glass and optical fiber as was observed in our experiments. Some phase separation and clustering processes in  $\text{As}_2\text{Se}_3$  and  $\text{As}_2\text{S}_3$  rare earth doped glass were established by X-ray diffraction [10,11] and Raman spectroscopy methods [10,23]. Because for successful development of rare earth fiber optic amplifiers it is necessary to decrease the optical losses in the host glass using different technological procedures [24,25].

#### 4. Summary

The optical properties of praseodymium-doped glasses have attracted considerable attention recently for their potential application as optical amplifiers at 1.3 and 1.6  $\mu\text{m}$ . We report here optical absorption spectra and mid-infrared emission properties of  $\text{Pr}^{3+}$ -doped  $\text{As}_2\text{S}_3$  glasses at room temperature. Experimental results on optical absorption and photoluminescence of  $\text{As}_2\text{S}_3$  bulk glasses and fiber samples doped with rare-earth ions ( $\text{Pr}^{3+}$ ,  $\text{Sm}^{3+}$ ,  $\text{Er}^{3+}$  and  $\text{Dy}^{3+}$ ) are presented. Near the absorption edge the rare-earth impurities strongly affect the slope and the magnitude of the weak absorption tail. Fluorescence spectra of bulk samples and optical fibers of arsenic sulfide doped with different concentrations of  $\text{Pr}^{3+}$  and  $\text{Dy}^{3+}$  indicate on the presence of luminescent band located around 1300 and 1500 nm. These bands correspond to the electron transitions from the discrete levels ( ${}^6\text{F}_{7/2} \rightarrow {}^6\text{H}_{13/2}$  and  ${}^6\text{F}_{5/2} \rightarrow {}^6\text{H}_{11/2}$  for  $\text{Dy}^{3+}$ ) and ( ${}^1\text{G}_{4/1} \rightarrow {}^3\text{H}_6$  and  ${}^3\text{F}_3 \rightarrow {}^3\text{H}_4$  for  $\text{Pr}^{3+}$ , respectively), and which confirmed the presence of trivalent rare-earth ions in the glass matrix. The observed effects of rare-earth dopants on the  $\text{As}_2\text{S}_3$  glass are discussed in connection with the expected behavior of the impurities in the glass. The luminescence signal at 1.6  $\mu\text{m}$  exhibits a quite pronounced time decay under continuous excitation of pumping light beam 0.808  $\mu\text{m}$ .

#### Acknowledgement

This work has been supported by the INTAS under the Grant 99 – 01229.

#### References

- [1] D. Lezal, J. Optoelectron. Adv. Mater. **5**(1), 35 (2003).
- [2] X. Zhang, H. Ma, J. Lucas, J. Optoelectron. Adv. Mater. **5**(5), 1327 (2003).
- [3] S. G. Bishop, D. A. Turnbull, B. G. Aitken, J. of Non-Cryst. Solids **266&269**, 876 (2000).
- [4] Properties, Processing and Applications of Glass and Rare Earth Doped Glasses for Optical Fibers, Ed. D. Hewak, INSPEC, London, UK, 1998.
- [5] Erbium-Doped Fiber Amplifiers. Fundamentals and Technology. Eds. P.C. Becker, N. A. Olsson, I. R. Simpson, Academic Press, San Diego-London-Boston, 1999.
- [6] D. Lezal, J. Pedlikova, J. Zavadil, J. Optoelectron. Adv. Mater. **6**(1), 133 (2004).
- [7] D. L. Wood, J. Tauc, Phys. Rev. **B5**, 3144 (1972).
- [8] W. B. Jackson, S. M. Kelso, C. C. Tsai, J. W. Allen, S.-J. Oh, Phys. Rev. **B31**, 5187 (1985).
- [9] M. Popescu, A. Andriesh, V. Chiumach, M. Iovu, S. Shutov, D. Tsiuleanu. The Physics of Chalcogenide Glasses, Ed. Stiintifica Bucharest - I.E.P. Stiinta, Chisinau, 1996.
- [10] M. S. Iovu, S. D. Shutov, A. M. Andriesh, E. I. Kamitsos, C. P. E. Varsamis, D. Furniss, A. B. Seddon, M. Popescu. J. Optoelectron. Adv. Mater. **3**(2), 443 (2001).
- [11] A. Andriesh, M. Popescu, M. Iovu, V. Verlan, S. Shutov, M. Bulgaru, E. Colomeyco, S. Malcov, M. Leonovici, V. Mihai, M. Steflea, S. Zamfira, In: Proc. 18<sup>th</sup> Annual Semicond. Conf. CAS'95, Sinaia (Romania), Oct. 1995 (**Vol.1**, p.83).
- [12] J. Ihm, Solid State Commun. **53**, 293 (1985).
- [13] A. Andriesh, I. Culeac, V. Loghin, Pure Appl. Optics **1**, 91 (1992).



- 
- [14] P. Hari, C. Cheney, G. Leupke, S. Singh, N. Tolk, J. S. Sanghera, I. D. Aggarwal, *J. Non-Cryst. Sol.* **270**, 265 (2000),
- [15] L. B. Shaw, B. B. Harbison, B. Cole, J. S. Sanghera, I. D. Aggarwal, *Optics Express* **1**, 87 (1997).
- [16] Z. Ohishi, A. Mori, T. Kanamori, K. Fujiura, S. Sudo, *Appl. Phys. Letters* **65**, 13 (1994),
- [17] J. Kirchof, J. Kobelke, M. Scheffler, A. Schwuchow. *Electronics Letters* **32**, 1220 (1996).
- [18] D. A. Turnbull, S. G. Bishop, *J. Non-Cryst. Solids* **223**, 105 (1998).
- [19] D. A. Turnbull, B. G. Aitken, S. G. Bishop. *J. Non-Cryst. Solids* **244**, 260 (1999).
- [20] R. A. Street, *Adv. Physics* **25**, 397 (1976).
- [21] R. A. Street, N. F. Mott, *Phys. Rev. Letters* **35**, 1293 (1975).
- [22] N. F. Mott, E. A. Davis, R. A. Street, *Philos. Mag.* **32**, 961 (1975).
- [23] M. S. Iovu, E. I. Kamitsos, C. P. E. Varsamis, Abstract of 2-nd Int. Conf. on Material Science and Condensed Matter, Sept. 21-26, 2004, Chisinau, Moldova, p.74.
- [24] G. G. Devyatykh, M. F. Churbanov, I. V. Scripachev, G. E. Snopatin, E. M. Dianov, V. G. Plotnichenko, *J. Non-Cryst. Sol.* **256&257**, 318 (1999).
- [25] M. F. Churbanov, V. G. Shiryaev, I. V. Scripachev, G. E. Snopatin, V. V. Gerasimenko, S. V. Smetanin, I. E. Fadin, V. G. Plotnichenko, *J. Non-Cryst. Sol.* **284**, 146. (2001).